PLASMA DIAGNOSTICS

STUDY OF INPUT CHARACTERISTICSIONIZATION CHAMBER OF A TWO-STAGE QUASI-STATIONARY HIGH-CURRENT PLASMA ACCELERATOR

© 2025 V. S. Chernyshev *, K. M. Gutorov, V. L. Podkovyrov, A. A. Mamonov

State Scientific Center of the Russian Federation "Troitsk Institute of Innovative and Thermonuclear Research" Troitsk, Moscow, Russia

**e-mail: chernyshev.valentin@triniti.ru*

Received November 25, 2024

Revised January 13, 2025

Accepted January 15, 2025

Abstract. At JSC SRC RF TRINITI, within the framework of the federal project "Development of technologies for controlled thermonuclear fusion and innovative plasma technologies", work is underway to create a prototype of a plasma rocket engine based on a two-stage quasi-stationary high-current plasma accelerator with separation of the processes of preliminary ionization of the working fluid and the final formation of a high-speed flow. The discharge characteristics of the input ionization chamber have been determined when using hydrogen and helium as the working gas in the current flow rate range of 1.5–3 mg per pulse, based on which recommended values of specific energy input in the range of 2.2–2.6 kJ/mg for H2 and 1.2–1.6 kJ/mg for He have been established. The plasma temperature estimate for hydrogen at a level of 0.8 eV is consistent with the measured plasma flow velocity 16 ± 3 km/s. The conversion factor of the input electrical energy into plasma flow energy was 65% over the entire range studied. The results obtained allow us to predict the electric discharge characteristics, cooling requirements, and erosion rate for the first stage of a plasma rocket engine.

Keywords: *quasi-stationary high-current plasma accelerator, plasma rocket engine*

DOI: 10.31857/S03672921250102e8

1. INTRODUCTION

At JSC "SSC RF TRINITI", as part of the implementation of the federal project "Development of Controlled Thermonuclear Fusion Technologies and Innovative Plasma Technologies" FP-3 of the comprehensive program "Development of Equipment, Technologies and Scientific Research in the Field of Nuclear Energy Use in the Russian Federation for the Period up to 2024" [1], work is being carried out to create a prototype of a plasma rocket engine based on a quasi-stationary high-current plasma accelerator (QSHPA). The concept of a two-stage QSHPA

is being implemented with separation of the processes of preliminary ionization of the working fluid and final formation of the high-speed flow. The basic principles of such installations were developed by Morozov A.I. [2, 3], one of their distinctive features is the presence of the first ionizing stage — an inlet ionization unit, usually consisting of several inlet ionization chambers (IIC). The main function of the IIC is complete ionization of the injected gas and regulation of plasma parameters at the entrance of the accelerating stage of the QSHPA. Numerical modeling of the acceleration channel demonstrates the importance of proper plasma feeding at the inlet [4–7] to avoid such problems as discharge non-stationarity [4, 5], ionization instability [5, 6], non-uniform current distribution on electrodes, up to the appearance of reverse currents (current vortices) [7]. It should be noted that there are no works on end-to-end modeling of both accelerator stages simultaneously. An approach is known with a separate calculation of the flow in the IIC and subsequent use of these results as input conditions for the acceleration stage [7]. The use of preliminary ionization in creating a prototype of a plasma rocket engine allows separating the processes of ionization and acceleration for their independent optimization, which should contribute to increasing the engine efficiency and electrode lifetime. The use of hydrogen as a working fluid is justified by the high energy efficiency of QSHPA operation on light gases and the target specific impulse of 100 km/s, at which the kinetic energy of a proton is 52 eV, which is not less than 70% of the total energy carried away by the flow per ion.

Two-stage KPSE were extensively studied experimentally in the late 80s and early 90s of the last century as part of a cooperation led by A.I. Morozov at the branch of the Kurchatov Institute (now TRINITI) [8], KhPTI (Kharkov) [9-11], MAI [12], Bauman Moscow State Technical University [13], and the Institute of Molecular and Atomic Physics (Minsk) [14]. Subsequently, the two-stage system was actively studied only at KhPTI [11]. Using such two-stage configurations, high plasma densities (10^{21}–10^{22} m $^{-3}$) and output flow velocities (10^{4}–10^{5} m/s) were achieved. The paper [10] presents the first results of the operation of such installations. An inductive storage was used as a power sharpener, and 6 PIC units were used to ensure the necessary symmetry and parameters of the plasma flow at the entrance to the acceleration channel. At KhPTI [11], studies were conducted at the same time with a similar two-stage installation with four PICs for gas ionization and generation of plasma flow with a velocity that ensures coordination of the two accelerator stages without disrupting the regularity of plasma flow. Velocity dependencies on discharge current and mass flow rate were obtained. The maximum velocity, measured by the time-

of-flight method, reached $7 \cdot 10^4$ m/s. At the same time, there were operating modes in which there was no near-electrode potential jump. Data on PIC electrode erosion are provided in [10], where its presence is noted only at discharge currents above 60 kA.

A targeted and detailed study of the IIC operation, allowing to choose the operating mode of the pre-ionization system for a new accelerator, has not been presented in any of the literature sources. Data for analysis from various installations had to be brought to unified analyzable values. The current value for the ongoing work on creating a prototype plasma rocket engine is a total gas flow rate of 6 mg with a current pulse duration of about 2 ms, which when using 4 IICs in the first stage gives an instantaneous flow rate of 0.75 g/s per single IIC. The minimum value of specific energy input into the discharge can be taken as 1.3 kJ/mg, based on the ionization potential of hydrogen, which is 13.6 eV. Table 1 shows the characteristic values for the first stage of the accelerator, obtained based on the experimental data presented in the literature: the value of the specific energy input was "reconstructed" from the available discharge characteristics (dependencies of current and discharge voltage), and the instantaneous gas flow rate was calculated from the total flow rate and pulse duration.

From the data presented, it is evident that all works were conducted with instantaneous flow rates significantly exceeding the current requirements, and complete ionization of the working medium (hydrogen) could only be achieved in narrow ranges of experimental conditions. In this regard, research is needed on IIC with the required instantaneous flow rate of the working medium and achieving sufficient energy input for complete ionization. This work is devoted to the study of operating modes of the input ionization chamber of a two-stage quasi-stationary plasma accelerator using hydrogen and helium as working gases in order to identify conditions for complete ionization of the working medium, determine the efficiency of energy input into the discharge and its upper limit, determined by erosion of the electrode system.

2. EXPERIMENTAL TECHNIQUE

The design of the VAT under study is a coaxial electrode system with a steel anode 7 cm in diameter and a profiled copper cathode with a maximum diameter of 5 cm. A pulsed electromagnetic valve is used to supply the working medium to the interelectrode space. The discharge is powered by a capacitor bank with a capacity of 16 mF with a maximum voltage of 5 kV, charged in experiments with VAT not higher than 2.4 kV. An inductance of 6 μH is connected

in series in the power circuit to match the shape of the current pulse with the shape of the gas pulse. This power supply scheme allows for regulating the current amplitude in the discharge circuit by changing the charging voltage of the battery. The residual pressure in the vacuum chamber is about 0.013 Pa, the total volume of the chamber is 6.5 m^3. Figure 1 shows the experimental setup with VAT (the electrode system is highlighted in brown) indicating the location of key diagnostics.

The discharge current and the carry-out current are measured using Rogowski coils (right and left belts in Fig. 1, respectively), and the discharge voltage is measured using a resistive divider. The total energy carried out by the plasma flow is measured using a copper calorimeter [15]. Light collection for spectral diagnostics is carried out via collimators installed perpendicular to the direction of flow and at an angle of 49.6 °, as shown in Fig. 1. Overview spectra are recorded in selected time intervals of the discharge with an accumulation duration of 11 μs, and high-speed registration of the H_α line is carried out to determine the flow velocity by the Doppler shift [16]. Visual observation of the flow is conducted using a Phantom 2512 high-speed camera with a frame exposure duration of 1 μs and a typical shooting speed of 62 000 frames/s. Figure 2 shows a frame illustrating the plasma flow exiting the electrode system and entering the calorimeter.

Each series of experiments is preceded by valve adjustment to ensure the necessary flow rate for each gas type. The instantaneous gas flow rate during valve operation is determined by the dynamic pressure value of the flow, measured by the PIEZOTRONICS 113B28 sensor at the critical section (the narrowest point of the electrode system). The characteristic time dependence of pressure is presented in Fig. 3 together with a similar dependence of the discharge current, which illustrates the consistency of current flow with gas supply to the discharge. The total pulse duration is close to 2 ms. The integral mass gas flow per pulse is determined in each run based on the pressure differential before and after the run in the buffer volume isolated from the supply line before the valve.

3. EXPERIMENTAL RESULTS

Studies have been conducted for two plasma-forming gases: H_2 and He. The gas flow rate varied in the range from 1 to 4 mg. The range of voltage variation on the discharge power capacitor bank: 0.8–2.4 kV.

Characteristic profiles of the discharge current and VCG voltage for hydrogen are presented in Fig. 4; for helium, similar characteristic time dependencies are observed. The current profile is

determined by the battery capacity and the power circuit inductance. The voltage profile reflects plasma parameters in the discharge gap at a given current. The effective resistance graph (ratio of voltage to discharge current) allows demonstrating the quasi-stationary discharge phase — an area where resistance can be considered constant. It can be seen that most of the discharge refers to the quasi-stationary phase, while the transient processes at the start and end occupy a smaller part in duration and, more importantly, in the energy invested during this time. Further, when plotting dependencies for all quantities (current, voltage, resistance), values are taken at the time corresponding to the current maximum. The carry-over current is the current flowing between the cathode and the vacuum chamber walls outside the main discharge gap and measured by a Rogowski coil placed around the anode. The carry-over current does not directly contribute to the ionization and heating processes occurring in the discharge gap, therefore, when plotting current dependencies and estimating the discharge voltage, only the part of the discharge current flowing in the electrode system (total current minus the carry-over current) was taken into account.

Current-voltage characteristics of the discharge are shown in Fig. 5. The results were obtained in the current range from 5 to 35 kA, with corresponding discharge voltage values from 100 to 300 V. The relative error in current measurement is 2% (calibration error of the Rogowski coil) and 9% in voltage measurement (determined by the error in selecting the voltage value at the maximum current). The lines of voltage versus current dependencies for two gases and two flow rates in the area of maximum currents of 25-35 kA converge to a single straight line (Fig. 5). The presented results qualitatively agree with the data in [17] in that the current-voltage characteristic of the heavier gas lies below that of the lighter one (in the source H_2 and N_2) in the current range from 20 to 50 kA and gas flow rates of about 1.5 g/s. For the two presented flow rate values and the presented current range, no sharp increase in discharge voltage with increasing current was observed, similar to the published data [17].

To bring the results with different mass flow rates to a single comparison parameter, the dependence of the discharge voltage on the specific energy input is plotted (Fig. 6). The specific energy input is calculated as the ratio of the total energy input into the discharge Q_d to the total gas flow rate in the pulse. Q_d is determined by integrating the product of the discharge current oscillograms I_d and discharge voltage U_d

$$Q_{\mathrm{d}} = \int_0^{\Delta t} I_{\mathrm{d}}(t) U_{\mathrm{d}}(t)\, dt, \qquad (1)$$

where Δt τ is the duration of the discharge pulse. The relative error in determining the energy input was 3%.

The most universal appears to be the dependence of the discharge resistance on the specific energy input (Fig. 7). One can set the minimum energy required for gas ionization based on the ionization potential without accounting for efficiency: 1.3 kJ/mg for H_2 and 0.59 kJ/mg for He. In Fig. 7 there are areas of decreasing resistance with increasing energy input and moments of reaching the minimum are determined, corresponding to complete gas ionization: 2.2–2.6 kJ/mg for H_2 and 1.2–1.6 kJ/mg for He. For He, an area of resistance growth is observed, which is associated with an increase in flow rate. Also significant is the fact that the resistance is independent of gas type and flow rate at specific energy inputs above 2.2 kJ/mg. It is assumed that this may be related to electrode erosion, leading to the introduction of heavy particles into the plasma, which prevents further increase in flow velocity. At a total discharge energy above 5 kJ, the thermal load on the cathode may exceed the melting threshold, which for copper is 0.7 MJ/m^2. Local melting marks were indeed observed on the cathode. The experiment also showed an increase in the intensity of copper lines at high energy input into the discharge.

Plasma flow calorimetry allows determining the efficiency of energy expenditure for plasma creation. The energy conversion coefficient is determined experimentally - the ratio of the total energy recorded by the calorimeter to the value of the total energy invested in the discharge Q_d. Figure 8 shows the dependence of the energy conversion coefficient on the total energy input into the discharge for hydrogen. The error is due to uneven cooling of thermocouples (plasma impact on the calorimeter cone), as well as the software processing procedure. The median value of the coefficient is 0.65, which can be interpreted as the energy cost of a hydrogen ion at the level of 20 eV/ion or the necessary ionization costs at the level of 2 kJ/mg. This result allows determining the amount of energy going to heat the VIK structure during its operation, as well as calculating cooling requirements.

Overview spectrum of plasma flow for hydrogen (Fig. 9) demonstrates predominantly the emission of Balmer series lines; among impurities, oxygen emission is most intense (unresolved triplet O I 777.2 / 777.4 / 777.5 nm is marked on the figure with the central wavelength), and weak copper lines (cathode material) can also be detected. Increasing the energy input generally leads to an increase in the intensity of H_β relative to H_α and enhancement of impurity emission.

Determination of the plasma flow velocity is performed by measuring the Doppler shift of the H_α spectral line when collecting the flow radiation with collimators installed for observation perpendicular to and following the escaping flow. The measurement methodology is described in detail in paper [16]. The characteristic time dependence of the velocity for energy input above 2 kJ/mg is shown in Fig. 10. The average velocity is about 16 ± 3 km/s. The error is due to the accuracy of determining the line maximum when processing a rather wide H_α contour. A velocity drop is observed at about 1.5 ms from the discharge start, which corresponds to a decrease in discharge power by approximately 4 times from the maximum.

4. ANALYSIS OF RESULTS

The discharge voltage (as well as effective resistance) can be estimated based on the geometric dimensions and plasma parameters of the VIC, using Ohm's law taking into account the azimuthal magnetic field **B**, radial current **j**, and longitudinal plasma velocity **u** [18] (Fig. 11)

$$\mathbf{E} = \frac{\mathbf{j}}{\sigma} - \frac{1}{c}[\mathbf{u} \times \mathbf{B}]. \qquad (2)$$

Most of the discharge current flows between the electrodes in a plasma layer about 1 cm wide behind the narrowest part of the interelectrode channel. To estimate plasma parameters, one can use characteristic values: ion and electron temperatures equal to $T_e = T_i = 1$ эВ , discharge current $I = 20$ кА , hydrogen consumption 3 mg per pulse, cross-sectional area of the discharge channel 30 cm ^{2}. The average thermal velocity of ions will be $1.56 \cdot 10^4$ m/s, electron velocity $6.7 \cdot 10^5$ m/s . Plasma concentration when ions escape with average thermal velocity $n = 7.56 \cdot 10^{16}$ см$^{-3}$. Debye radius $r_D = 2.7 \cdot 10^{-8}$ m. Length and time of Coulomb scattering of electrons on ions: $\lambda_{ei} = 1.14 \cdot 10^{-6}$ m, $t_{ei} = 1.9 \cdot 10^{-12}$ s. With such a small electron mean free path, the assumption of equality between the electron and ion temperature components ($T_e = T_i$) is valid. The ohmic resistance of the plasma layer is 3.7 mOhm, and the corresponding ohmic voltage component is $U_r = 75$ V.

Plasma movement in a magnetic field generated by current flowing through electrodes leads to multidirectional displacement of ions and electrons, increasing the voltage between electrodes. The magnetic field induction at the cathode is $B_c = I/(2\pi r_c) = 0.25$ T, where r_c is the cathode

radius. When hydrogen plasma moves at a speed of 15.6 km/s, the Lorentz component of the voltage equals $U_{Lor} = 74$ V. Estimates of the Hall parameter for electrons and ions give $\chi_e = 0.15$ and $\chi_i = 8 \cdot 10^{-5}$ respectively, which indicates the absence of magnetization for both ions and electrons. Electron magnetization would be possible with decreased plasma density, for example, by increasing the installation dimensions or using a heavier plasma-forming gas.

The results of discharge parameter estimation in H_2 and He for two plasma temperature values, as well as the corresponding experimental results, are shown in Table 2. Two close values of discharge current were selected (26.5 kA for H_2 and 27.5 kA for He), corresponding to the minimum values of effective discharge resistance. To calculate the ohmic component of voltage, U_r the portion of discharge current flowing in the electrode system was used (total current minus the carryover current), while the total current was used in the magnetic field calculation. "Estimate 1" was performed for the temperature value at which complete ionization should be achieved assuming thermodynamic equilibrium (i.e., assuming the applicability of the Saha equation). The ohmic voltage component in this case turns out to be greater than the Lorentz component, and the total effective resistance is overestimated compared to experimental data. "Estimate 2" was performed for a temperature value selected to achieve equality of the two voltage components, which should correspond to the minimum effective resistance, which turns out to be close in magnitude to the experimental data. These are the values shown by lines for the calculated resistance in Fig. 7. Flow velocity measurement results also indicate a plasma temperature close to 1 eV.

The balance of the ohmic and Lorentz components of voltage strongly depends on plasma temperature. At low temperature, the ohmic component of voltage is significantly greater than the Lorentz component; however, as temperature increases with increasing energy input, this difference substantially decreases because $U_{Lor} \sim \sqrt{T}$, and $U_r \sim T^{-3/2}$. At sufficiently high temperature or high velocity, a situation may occur where the ohmic component is lower than the Lorentz component.

The effective resistance for helium in the considered current range turns out to be lower than for hydrogen. This is due to the significantly lower outflow velocity of helium - at the same temperature, the velocity is 2 times lower due to the 4-fold difference in mass, which is reflected in the lag in the magnitude of the Lorentz component $U_{Lor} \sim u_i \sim m_i^{1/2}$ (95 V - H_2 and 52 V - He).

The ohmic component, which depends on ion mass as $U_r \sim Ln(m_i)$ will be somewhat higher in magnitude for helium at equal temperatures (81 V - H_2 and 86 V - He). With an increase in gas mass flow rate, the total voltage increases due to an increase in the ohmic component. It's worth noting that for an arc discharge, the magnitude of the near-cathode potential drop can be estimated as the ionization potential of the corresponding gas. Thus, the near-cathode potential drop for hydrogen does not exceed 13.6 V, and for helium - 24.59 V, which increases the total voltage when working with helium.

5. CONCLUSION

The discharge characteristics of the input ionization chamber of a two-stage quasi-stationary plasma accelerator have been determined when using hydrogen and helium as working gases in the range of 1.5-3 mg per pulse, which is relevant for creating a prototype plasma rocket engine. The use of inductance in the discharge circuit made it possible to delay the current rise front and coordinate the discharge current flow with the dynamics of gas entry into the interelectrode gap.

Analysis of the discharge effective resistance behavior as a function of specific energy input allows to identify characteristic transition regions from a state dominated by the ohmic voltage component to a state dominated by the Lorentz component. The plasma temperature estimate in the resistance minimum region for hydrogen at the level of 0.8 eV is consistent with the measured plasma flow velocity of 16 ± 3 km/s. The low effective resistance for helium compared to hydrogen in the low energy input region is explained by a significantly lower outflow velocity, leading to a small value of the Lorentz component in the discharge voltage. At energy inputs above 2.6 kJ/mg, constant effective resistance is observed with the same value for both hydrogen and helium, while the intensity of impurity lines increases in the discharge emission spectrum. These signs indicate the influx of cathode material vapors into the discharge, which should be avoided. The presented results allow recommending the HPC operation with energy input in the range of 2.2–2.6 kJ/mg for H_2 and 1.2–1.6 kJ/mg for He.

Calorimetry data provide a conversion coefficient of the input electrical energy into plasma flow energy of 65% throughout the entire investigated range. The obtained results allow predicting electrical discharge characteristics, cooling requirements, and erosion rate for the first stage of a plasma rocket engine based on a quasi-stationary high-current plasma accelerator.

FUNDING

This work was carried out under the state contract No. N.4k.241.09.23.1062 dated 04/19/2023.

REFERENCES

1. *Ilgisonis V.I., Ilyin K.I., Novikov S.G., Olenin Yu.A* . // Plasma Physics. 2021. V. 47. P. 963.
2. *Morozov A.I.* // UFN. 1990. V. 160. P. 147.
3. *Morozov A.I.* // Plasma Physics. 1990. V. 16. P. 131.
4. *Kozlov A.N.* // Phys. Fluids. 2022. V. 34. P. 104109. Doi: 10.1063/5.0117298
5. *Kozlov A.N., Klimov N.S., Konovalov V.S., Podkovyrov V.L., Urlova R.V.* // J. Phys.: Confer. Ser., 18th Internat. Workshop Magneto-Plasma Aerodynamics. 2019. P. 012021. Doi: 10.1088/1742-6596/1394/1/012021.
6. *Brushlinsky K.V., Morozov A.I.* Problems of Plasma Theory. Issue 8 / Ed. by M. A. Leontovich. Moscow: Gosatomizdat, 1974. P. 88.
7. *Brushlinsky K.V., Zaborov A.M., Kozlov A.N., Morozov A.I., Savelyev V.V.* // Plasma Physics. 1990. Vol. 16. P. 147.
8. *Belan V.G., Zolotarev S.P., Levashov V.F., Mainashev V.S., Morozov A.I., Podkovyrov V.L., Skvortsov Yu.V* . // Plasma Physics. 1990. Vol. 16. P. 176.
9. *Voloshko A.Yu., Garkusha I.E., Kazakov O.E., Morozov A.I., Pavlichenko O.S., Solyakov D.G., Tereshin V.I., Tiarov M.A., Trubchaninov S.A., Tsarenko A.V., Chebotarev V.V.* // Plasma Physics. 1990. Vol. 16. P. 158.
10. *Staltsov V.V., Makhlay V.A., Chebotarev V.V., Kulik N.V.* // Instruments and Experimental Techniques. 2019. No. 4. P. 73.
11. *Garkusha I.E., Solyakov D.G., Chebotarev V.V., Makhlay V.A., Kulik N.V.* // Plasma Physics. 2019. Vol. 45. P. 179.
12. *Dyakonov G.A., Tikhonov V.B.* // Plasma Physics. 1994. Vol. 20. No. 6. P. 533.
13. *Mastyukov E.N., Mishanov A.V., Khvesyuk V.I.* // Abstracts of the VII All-Union Conference on Plasma Accelerators and Ion Injectors. Kharkov, 1989. P. 45.
14. *Ananin S.I., Astashinsky V.M., Bakanovich G.I., Kostyukevich E.A., Kuzmitsky A.M., Mankovsky A.A., Minko L.Ya., Morozov A.I.* // Plasma Physics. 1990. Vol. 16. P. 186.

15. *Klimov N.S., Kovalenko D.V., Podkovyrov V.L., Kochnev D.M., Yaroshevskaya A.D., Urlova R.V., Kozlov A.N., Konovalov V.S.* // VANT. Ser. Thermonuclear Fusion. 2019. Vol. 42. P. 52.

Doi: 10.21517/0202-3822-2019-42-3-52-63.

16. *Yaroshevskaya A.D., Gutorov K.M., Podkovyrov V.L., Litvinenko Yu.I* . // Plasma Phys. Rep. 2024. V. 50. P. 689.

Doi: 10.1134/S1063780X24600634

17. *Kovrov P.E., Shubin A.P*. Physics and Application of Plasma Accelerators / Ed. by A.I. Morozov. Minsk: Science and Technology, 1974. P. 78.

18. *Morozov A.I., Solovyev L.S*. Reviews of Plasma Physics. Issue 8 / Ed. by M.A. Leontovich. Moscow: Gosatomizdat, 1974. P. 3.

Table 1. Characteristic values of specific energy input into the VIK discharge for hydrogen.

Installation	Specific energy input, kJ/mg	Gas consumption, mg	Pulse duration, ms	Instantaneous gas flow rate, g/s
KSPU-P50 [8]	0.24	30.0	1.00	30.00
KSPU-Kh50 [9]	0.39–3.50	0.75	0.25	3.00
	0.04–0.57	5.00	0.25	20.00
KSPU-Kh50 [10]	0.07–3.07	0.45	0.24	1.88
	0.02–0.92	1.35	0.24	5.63

Table 2. Comparison of experimental and calculated data for H_2 and He at instantaneous flow rate of 1.5 g/s

	H_2			He		
	Experiment	Estimate 1	Estimate 2	Experiment	Estimate 1	Estimate 2
I,A	26.5			27.5		
T, эВ	–	0.21	0.8	–	0.35	1.4
U, В	242	397	249	165	353	154
U_r, В	–	334	125	_	315	77
U_{Lor}, В	–	63	124	–	38	77
R_{eff}, мОм	9.1	15	9.4	6	12.8	5.6

FIGURE CAPTIONS

Рис. 1. Scheme of experiments with input ionization chamber.

Рис. 2. Frame with image of plasma flow entering the calorimeter.

Рис. 3. Matching profiles of discharge current and dynamic gas pressure for hydrogen (for helium, the dependence has a similar appearance)

Рис. 4. Characteristic time dependencies of discharge current and carry-out current, voltage and discharge resistance for hydrogen

Рис. 5. Current-voltage characteristics of discharge for H_2 and He gases at flow rates of 1.5 and 3.0 mg.

Рис. 6. Dependence of discharge voltage on specific energy input for H_2 and He gases at flow rates of 1.5 and 3.0 mg.

Рис. 7. Dependence of discharge resistance on specific energy input for H_2 and He gases at flow rates of 1.5 and 3.0 mg. Horizontal lines show the calculated value according to "Estimate 2" from Table 2.

Рис. 8. Dependence of energy conversion coefficient on total energy input into discharge for hydrogen.

Рис. 9. Overview spectrum of plasma flow for hydrogen.

Рис. 10. Time dependence of plasma flow velocity.

Рис. 11. Illustration of discharge in input ionization chamber.

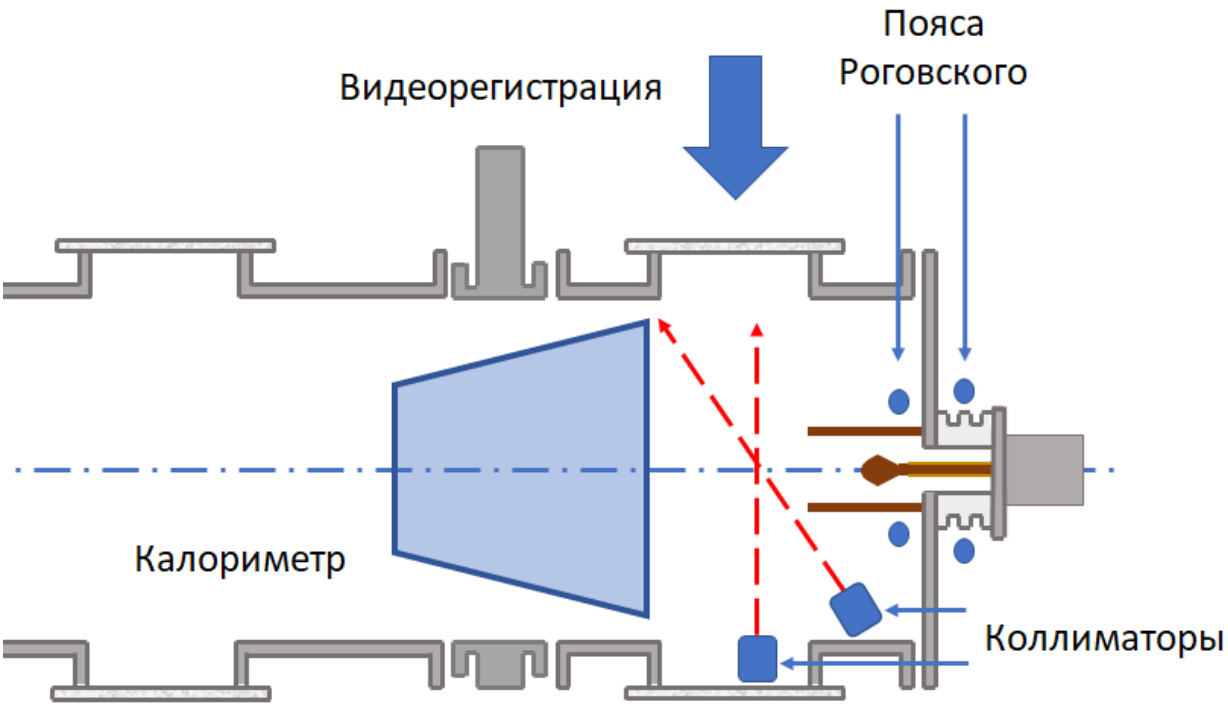
Пояса
Роговского
Видеорегистрация
Калориметр
Коллиматоры

Fig. 1

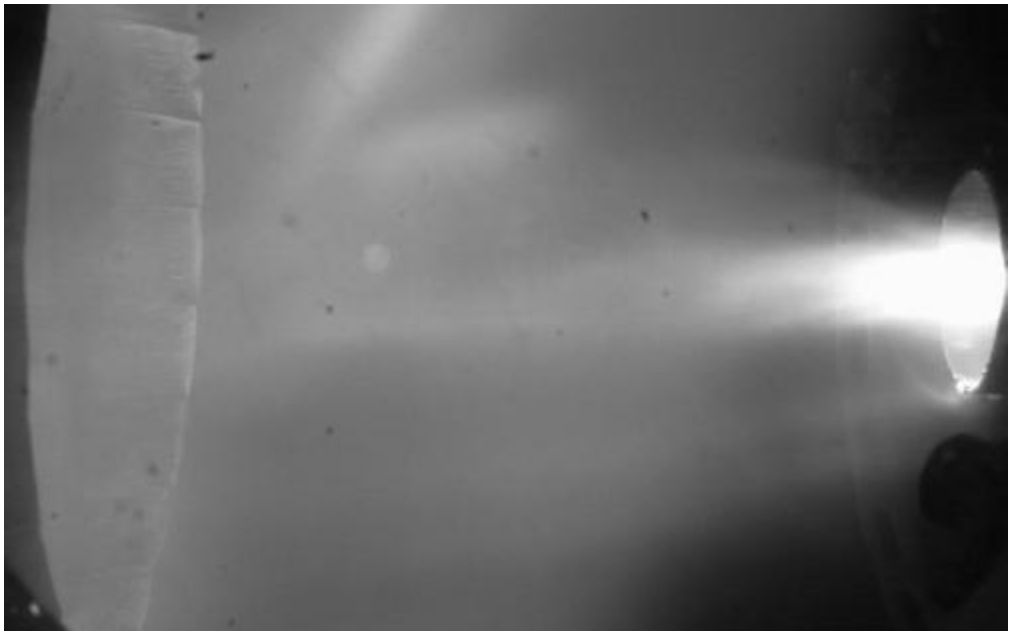

Fig. 2


Ток разряда, кА
Давление, кПа
Время от начала разряда, мс

Fig. 3

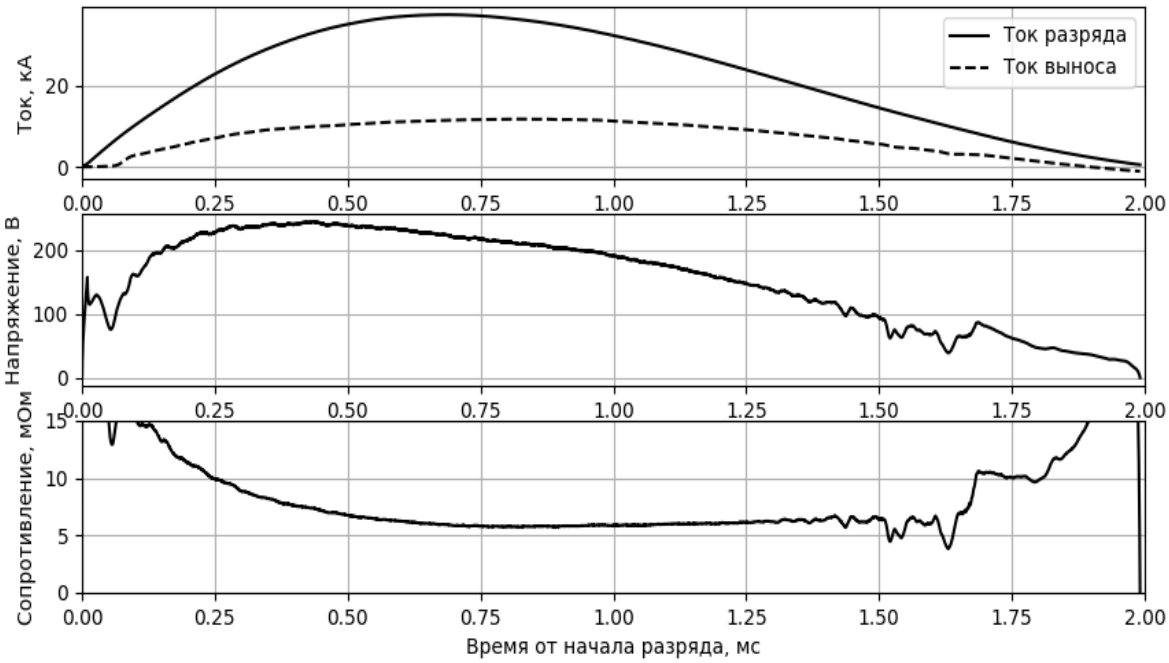
Ток разряда
Ток выноса
Ток, кА
Напряжение, В
Сопротивление, мОм
Время от начала разряда, мс

Fig. 4

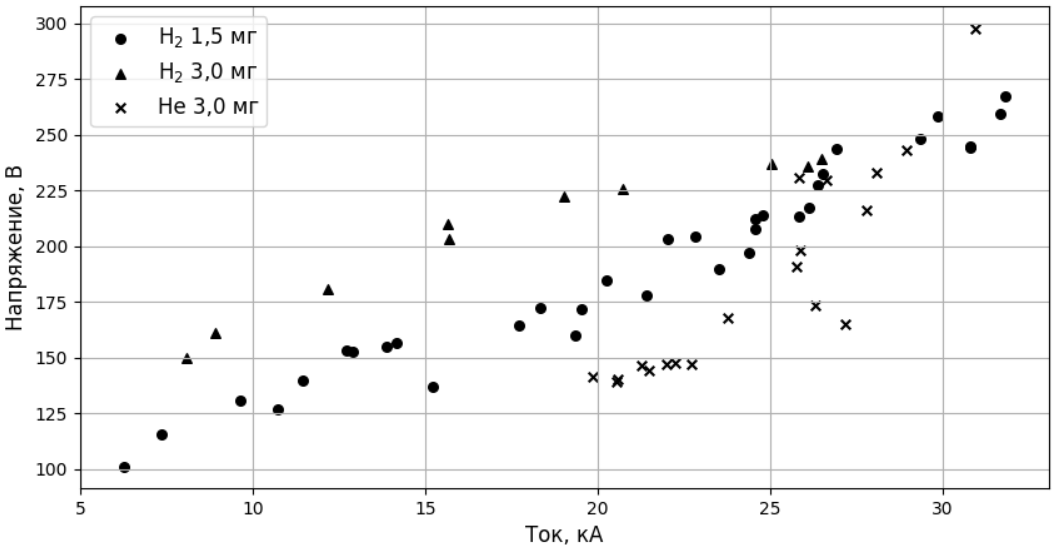
H2 1,5 мг
H2 3,0 мг
He 3,0 мг
Напряжение, В
Ток, кА

Fig. 5

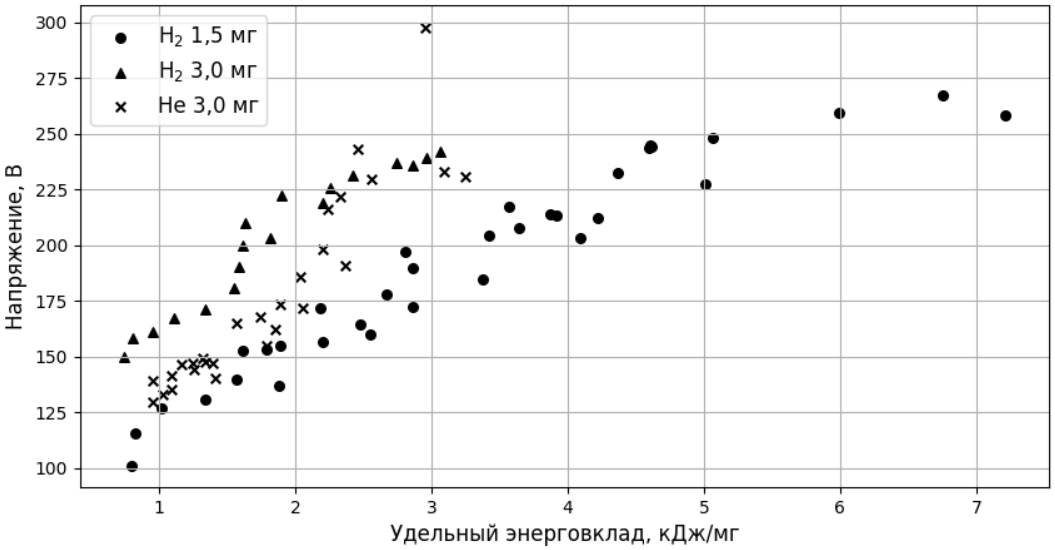
H2 1,5 мг
H2 3,0 мг
He 3,0 мг
Напряжение, В
Удельный энерговклад, кДж/мг

Fig.6

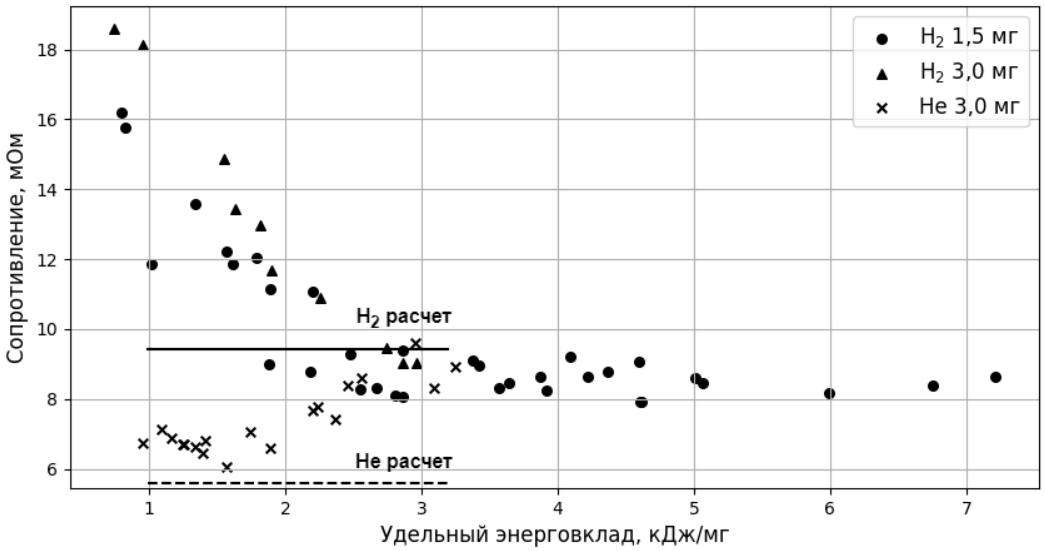
H2 1,5 мг
H2 3,0 мг
He 3,0 мг
H2 расчет
He расчет
Сопротивление, мОм
Удельный энерговклад, кДж/мг

Fig. 7

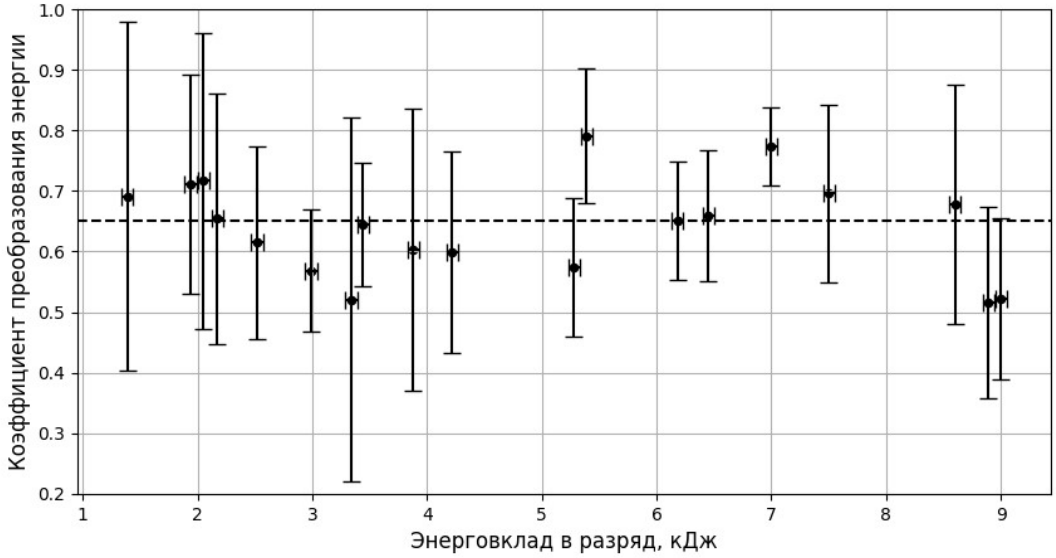
Коэффициент преобразования энергии
Энерговклад в разряд, кДж

Fig. 8

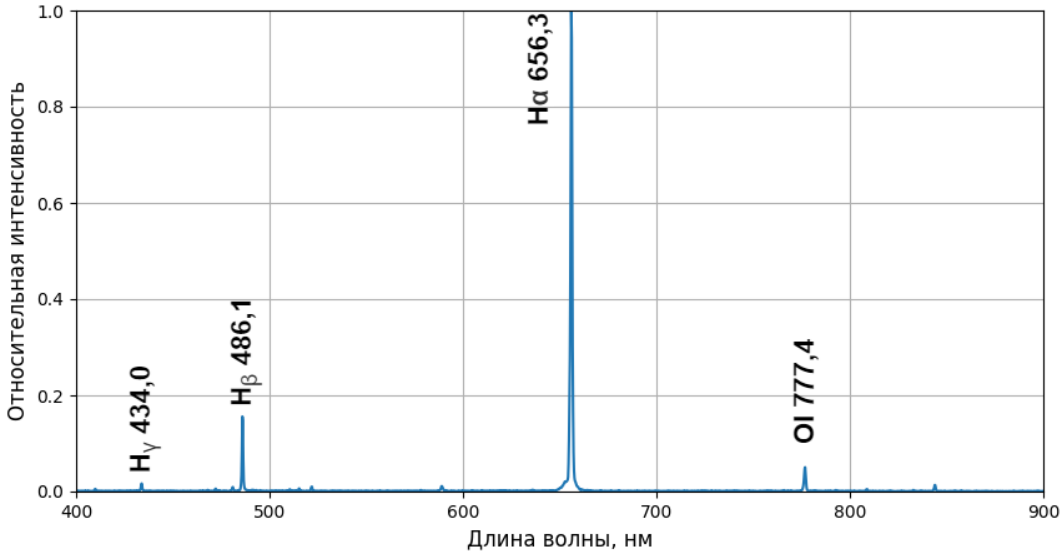
Относительная интенсивность
Длина волны, нм
Hα 656,3
Hβ 486,1
Hγ 434,0
OI 777,4

Fig. 9

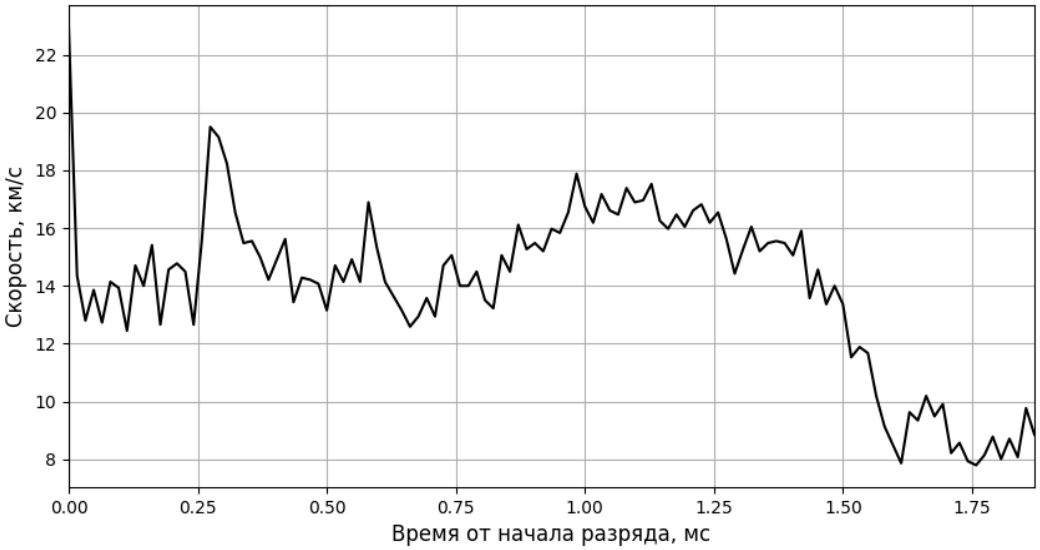
Скорость, км/с
Время от начала разряда, мс

Fig. 10

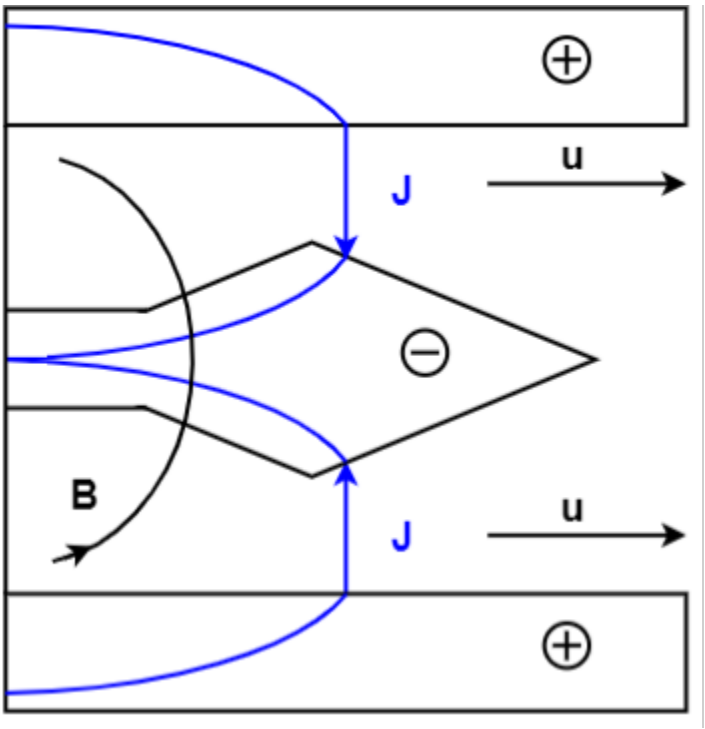

Fig. 11